

Ligand Design

Phosphorescent Platinum(II) Complexes with C^{AC*} Cyclometalated NHC Dibenzofuranyl Ligands: Impact of Different Binding Modes on the Decay Time of the Excited State

Alexander Tronnier,^[a] Gerhard Wagenblast,^[b] Ingo Münster,^[b] and Thomas Strassner*^[a]

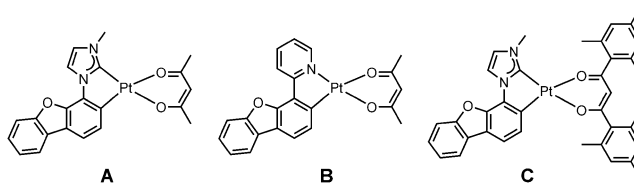
Abstract: Two C^{AC*} cyclometalated platinum(II) *N*-heterocyclic carbene (NHC) complexes with the general formula [(C^{AC*})Pt(O^{AO})] (C^{AC*}=1-dibenzofuranyl-3-methylbenzimidazolylidene; O^{AO}=dimesitoylethane) have been synthesized and extensively characterized, including solid-state structure determination, ¹⁹⁵Pt NMR spectroscopy, and 2D NMR (COSY, HSQC, HMBC, NOESY) spectroscopy to elucidate the impact of their structural differences. The two regioisomers differ in the way the dibenzofuranyl (DBF) moiety of the NHC ligand is bound to the metal center, which induces significant changes in their physicochemical properties, especially on the decay time of the excited state. Quantum yields of over 80% and blue emission colors were measured.

The concept of employing transition-metal complexes as phosphorescent emitter materials in organic light-emitting devices (OLEDs), utilizing their strong spin-orbit coupling (SOC) to enhance quantum yields and emission decay properties, has been extensively explored over the past decade.^[1] Quantum yields approaching unity and the ability to tune the emission color from the blue to near infrared region of the spectrum have triggered a rush in research towards cyclometalated complexes with heavy transition metals, especially iridium and platinum complexes.^[2] In 1998, Baldo et al. demonstrated the first device with a porphyrin-based platinum complex that exhibited red electrophosphorescence.^[3] Following these findings, research efforts shifted to heteroleptic cyclometalated Pt^{II} emitters with bidentate^[2b-e,4] or tridentate^[5] ligands. As such, pyridinyl, imidazolyl, or other five-membered heterocycles are a repeatedly found fragment used as neutral *N*-coordinated σ-donor ligands. Recently, these fragments were replaced by *N*-heterocyclic (NHC) ligands,^[6] leading to stronger ligand fields

and, thus, blueshifted emission maxima, addressing the still unfulfilled demand for stable blue emitters. The resulting complexes feature imidazole or benzimidazole moieties, allowing for well-directed fine-tuning of the electronic properties by modifying the *N*-bound substituents or incorporating electron-donating or -withdrawing groups in the NHC backbone.^[7]

Our group has reported different studies on bidentate C^{AC*} ligands, wherein the influence of modifications in the cyclometalated fragment, of extensions of the NHCs π-system, the use of triazole-based carbenes, and the impact of ancillary ligands, was investigated.^[7b-f,8] A complex (Scheme 1 A) bearing a dibenzofuranyl (DBF)-based NHC ligand together with the common monoanionic acetylacetonato (acac) ancillary ligand showed an outstanding quantum yield of 90%, a blue emission maximum (463 nm), but a relatively long decay lifetime of 23 μs in poly(methyl methacrylate) (PMMA) at room temperature (RT).^[9] First device tests showed very good external quantum efficiencies of 6.2% at 300 cd m⁻² and a maximum luminance of 6750 cd m⁻² considering that the stack design was not optimized. In contrast, similar complexes featuring pyridinyl instead of 3-methylimidazolylidene showed green emission (516 nm) and quantum yields of 43% (Scheme 1 B).^[10]

Replacing the acac ligand with a more bulky congener, namely, the dimesitoylethane (mesacac) ligand, led to increased solubility, reduced aggregation behavior, and an improvement of the photoluminescence properties to 91%, 466 nm, and 18.9 μs (Scheme 1 C).^[7c] Furthermore, we recently showed that an extension of the π-system in the rigid NHC backbone could increase the quantum yield.^[7e] In the present study we combine these earlier results in one system and investigate the influence of different ways of attaching the DBF fragment to the heterocyclic system and thus the metal center with the goal to reduce the decay lifetime, which remains a very critical aspect in overall device stability. In particular, the latter may inspire new ideas of how the established DBF fragment can be used in other cases.



Scheme 1. Platinum(II) complexes with cyclometalated DBF-NHC (A, C) and DBF-pyridinyl (B) ligands.

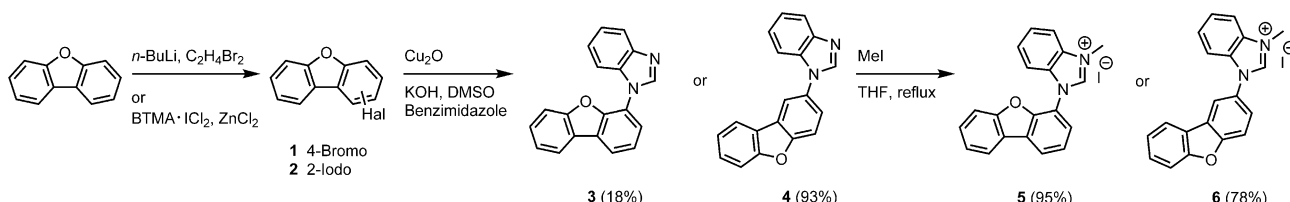
[a] Dr. A. Tronnier, Prof. Dr. T. Strassner

Physikalische Organische Chemie
Technische Universität Dresden
01069 Dresden (Germany)
E-mail: thomas.strassner@chemie.tu-dresden.de

[b] Dr. G. Wagenblast, Dr. I. Münster
BASF SE

67056 Ludwigshafen (Germany)

Supporting information for this article is available on the WWW under <http://dx.doi.org/10.1002/chem.201502087>.



Scheme 2. Synthesis of the NHC precursors **5** and **6** (yield).

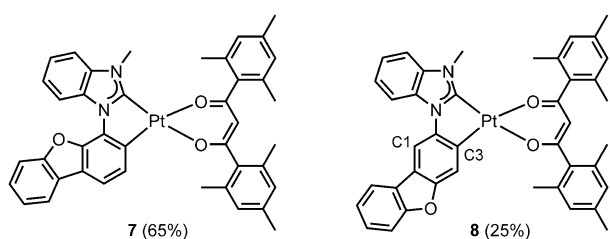
The synthesis of the ligand precursors started with the selective halogenation of dibenzofuran (Scheme 2). The bromination in the 4-position was achieved by deprotonation/lithiation at -40°C , followed by metal–halogen exchange at -78°C using 1,2-dibromoethane.^[9] Benzyl trimethyl ammonium dichloroiodate ($\text{BTMA}\cdot\text{ICl}_2$) and zinc chloride were used to facilitate an iodination in the 2-position. The halogenated dibenzofuranes **1** and **2** were subsequently coupled with benzimidazole in a copper(I)-catalyzed Ullmann-type reaction to generate the corresponding benzimidazoles **3** and **4** in low (18%) to very good (93%) yields. Finally, methylation was undertaken with an excess of iodomethane at elevated temperatures. The complexes were synthesized following our previously reported route.^[9] The imidazolium salts were reacted with silver(I) oxide, yielding a silver complex as intermediate, which was immediately transmetalated to the platinum(II) precursor dichloro(1,5-cyclooctadiene)platinum(II) ($\text{Pt}(\text{COD})\text{Cl}_2$). In the next step cyclo-metallation was achieved by heating to reflux for a prolonged time. Finally, the ancillary ligand mesacac and potassium *tert*-butanolate as a base were added to generate the products **7** and **8** in good to moderate yields (Scheme 3).

Both complexes were thoroughly characterized. The first significant difference between them was found by measuring the melting points. Whereas compound **7** melts at $232\text{--}234^\circ\text{C}$, isomer **8** has a melting point beyond 330°C . In the ^{195}Pt NMR spectra, complex **7** showed a signal at -3358 ppm in CDCl_3 and **8** one at -3320 ppm, whereas the values for the reference complexes **A** and **C** (Scheme 1) were reported as -3390 and -3341 ppm.^[7c,9] This difference in the chemical shifts already shows a slight effect of the DBF binding mode on the electron density at the metal center. 2D NMR experiments were conducted (see the Supporting Information, Figures S1–S10) to confirm the actual structure of complex **8**, as next to the C3–Pt configuration shown in Scheme 3, an isomer with a C1–Pt bond is possible, although disfavored according to DFT calculations. In this case, the DBF fragment would be rotated about

180° (see below, Figure 4). As a coupling between the hydrogen atom of the CH group surrounded by the C–Pt bond and the oxygen atom and a hydrogen atom from the *ortho*-CH₃ group of the mesetyl fragment from the ancillary ligand was observed, this result is only in agreement with the structure shown in Scheme 3.

For both complexes, single crystals suitable for X-ray diffraction experiments were grown to unambiguously confirm the 3D structures of the compounds (Figure 1). The results also confirmed the bonding situation of complex **8** with the platinum–carbon bond to be in the 3-position of the DBF fragment (see DFT section).

The metal atom is coordinated in a square-planar fashion. The shortest metal–ligand contact in complex **7** is found for the carbon–metal bond C9–Pt1 of the DBF fragment with $1.963(10)$ Å, which is marginally shorter than the C1–Pt1 bond ($1.966(14)$ Å). This surprising finding is the very first example for the whole class of bidentate C⁺C* cyclometalated NHC Pt^{II} complexes where the carbene carbon–metal bond is not distinctively the shortest metal-to-ligand bond.^[2a,7b–g,8,11] The picture for **8** is reversed, back to the previously observed trends with a C1–Pt1 distance of $1.926(8)$ Å and a C9–Pt1 bond length of $1.970(7)$ Å. Both complexes crystallized in the triclinic $P\bar{1}$ space group (see Supporting Information, Table S1), but with very different Pt···Pt distances and molecular interactions (see Supporting Information, Figure S11 and S12). In the structure of **8** the molecules are more intercalated, leading to shorter Pt···Pt distances of 6.76 to 9.31 Å and perpendicular separations between two neighboring molecules of 3.15 and 3.46 Å.



Scheme 3. C⁺C* cyclometalated complexes **7** and **8** (yield).

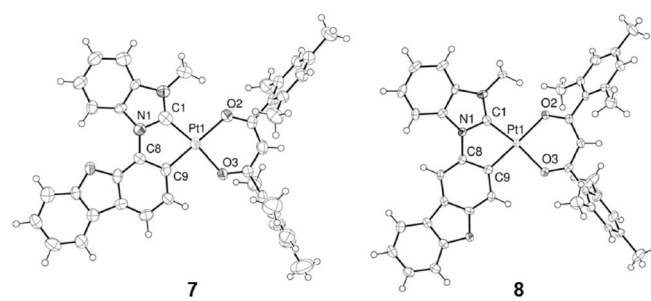


Figure 1. ORTEP representation of complexes **7** and **8** in the solid state. Thermal ellipsoids are drawn at the 50% probability level. Selected bond lengths (Å) and angles (°) for **7**: C1–Pt1, $1.966(14)$; C9–Pt1, $1.963(10)$; O2–Pt1, $2.101(8)$; O3–Pt1, $2.062(8)$; C1–Pt1–C9, $80.4(5)$; O2–Pt1–O3, $89.5(3)$; C8–N1–C1–Pt1, $2.1(12)$. For **8**: C1–Pt1, $1.926(8)$; C9–Pt1, $1.970(7)$; O2–Pt1, $2.082(5)$; O3–Pt1, $2.059(5)$; C1–Pt1–C9, $80.4(3)$; O2–Pt1–O3, $89.5(2)$; C8–N1–C1–Pt1, $-0.8(8)$.

From the experimental results discussed above, it is obvious that the actual binding mode from the metal to the DBF fragment has a significant impact on the properties of these compounds. This also holds true for their photophysical characteristics. Measurements with 2 wt% emitter in amorphous PMMA films show absorption between 240 and 340 nm at room temperature (see Supporting Information, Figure S13). The emission spectra, shown in Figure 2, clearly demonstrate the difference between **7** and **8**. Although both show an emission maximum at around 475 nm and a certain degree of vibronic coupling, complex **8** has a weaker first-emission band in the deep blue region at 450 nm and a less resolved spectrum. Thus, the Huang–Rhys ratio is $S > 1$, which would hint at geometrical distortions in the triplet state. For **7**, three distinctive bands (475, 506, and 542 nm) with a vibronic progression of 1290 and 1313 cm^{-1} are observed, leading to a bluish-green color (Table 1). Complex **8** shows only two discernible bands with a separation of 1345 cm^{-1} and a more pure blue color (CIE 0.175;0.268). High quantum yields of 84% (**7**) and 80% (**8**) were measured at room temperature in the diluted films and the decay lifetime of **8** ($10.8\text{ }\mu\text{s}$) is only half of that for **7** ($22.4\text{ }\mu\text{s}$). Experiments with pure amorphous emitter films showed additional significant differences between the regioisomers (Figure 3), namely, a remarkably high quantum yield of 31% for **7**, but only 4% for **8**, and the appearance of an additional unstructured band in the green-yellow region

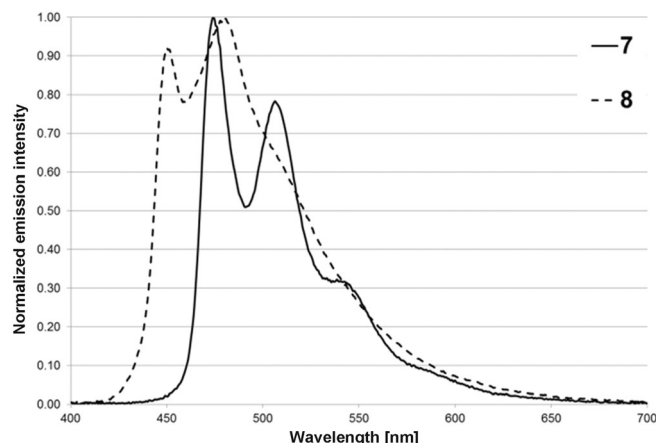


Figure 2. Emission spectra of **7** and **8** (2 wt% in PMMA, room temperature).

Table 1. Photoluminescence data (2 wt% in PMMA, room temperature) of the cyclometalated complexes **7** and **8** (λ in nm, τ in μs and k in 10^3 s^{-1}).

	$\lambda_{\text{exc}}^{[a]}$	$\text{CIE}^{[b]}$	$\lambda_{\text{em}}^{[c]}$	$\phi^{[d]}$	$\tau_o^{[e]}$	$k_r^{[f]}$	$k_{\text{nr}}^{[g]}$
7	370	0.180; 0.427	475	0.84	22.4	44.6	8.7
8	340	0.175; 0.268	479	0.80	10.8	92.7	23.3

[a] Excitation wavelength. [b] CIE $x:y$ coordinates at room temperature. [c] Maximum emission wavelength. [d] Quantum yield at λ_{exc} , N_2 atmosphere. [e] Decay lifetimes (excited by laser pulses (355 nm, 1 ns)) given as $\tau_o = \tau_v/\phi$. [f] $k_r = \phi/\tau_v$. [g] $k_{\text{nr}} = (1 - \phi)/\tau_v$.

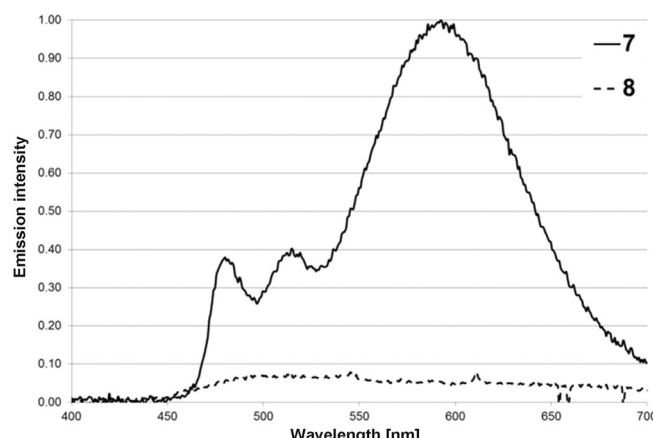


Figure 3. Emission spectra of **7** and **8** (100 wt% films at room temperature).

(592 nm) for **7**. This shifts the CIE coordinates to 0.477;0.462 and indicates intermolecular interactions. From both solid-state determination and DFT calculations, Pt–Pt interactions and a metal–metal-to-ligand charge transfer (MMLCT) are ruled out due to the steric demand of the mesacac ancillary ligand. Thus, the emission with a very short decay lifetime of $4.4\text{ }\mu\text{s}$ can only be explained by intermolecular π – π interactions made possible by the more extended π -system of the benzimidazole unit and the orientation of the DBF in **7**.

For complexes **7** and **8**, geometry optimizations were undertaken using DFT methods. The optimized structures for the singlet state show a nearly perpendicular orientation of the mesityl rings of the ancillary ligands and similar bond lengths to the X-ray diffraction experiments (see Supporting Information, Tables S2 and S3). Even at the transition to the triplet state, no rotation of the aryl substituents leading to a planarization were observed, due to the *ortho*-methyl groups of the mesityl moiety. Nonetheless, the observed Huang–Rhys ratio of $S > 1$ is validated by a slight distortion of the ancillary ligand in the case of **8**. A free-energy difference between the isomeric complexes **7** and **8** of only 2.2 kcal mol^{-1} was calculated, with **8** being thermodynamically favored. A possible third regioisomer, **8 iso** (Figure 4), which could, in principle, be formed during the synthesis of **8** was found to be 6.9 kcal mol^{-1} higher in free

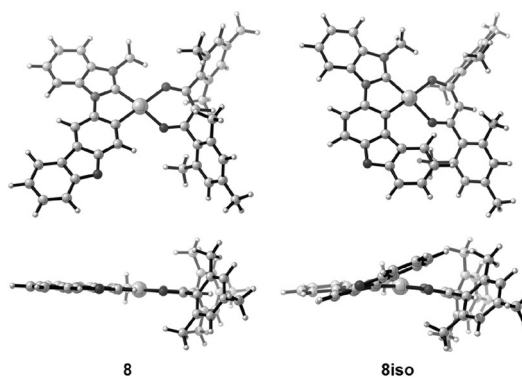


Figure 4. Optimized ground state structures of **8** (left) and the possible isomer **8 iso** (right, B3LYP/6-31G(d)).

energy, due to a strong distortion in the NHC ligand induced by steric interactions with the mesacac ligand. For more electronic evaluations, frontier molecular orbitals, and spin densities, see the Supporting Information, Figures S14 and S15.

Two novel platinum(II)-NHC complexes with a cyclometalated dibenzofuranyl unit were prepared and characterized. They are regioisomers in which the DBF moiety and the benzimidazol-2-yliden part of the NHC ligand are bonded in a different fashion. The isomer with the bond at the 2-position shows remarkable differences compared to the other compound. In particular, much faster emissive decay is observed, which is important for highly efficient OLEDs and improved device lifetimes. Although the mesacac ancillary ligand effectively prevents any Pt···Pt interactions apparent from the solid-state structures obtained from X-ray diffraction experiments, a bathochromic shift of the emission wavelength and high quantum yields were observed in pure emitter films of **7** that might arise from interligand interactions induced by π - π stacking made possible by the DBF orientation.

Acknowledgements

We are grateful to Dr. Breiten, Dr. Metz, and Dr. Lennartz (BASF SE) for helpful discussions. We also thank the ZIH for computation time on their high-performance computing facility and the BMBF (FKZ: 13N10477) for funding.

Keywords: carbene complexes • density functional calculations • ligand design • photophysics • X-ray diffraction

- [1] a) J. A. G. Williams, *Top. Curr. Chem.* **2007**, *281*, 205–268; b) H. Yersin, *Highly Efficient OLEDs with Phosphorescent Materials*, Wiley-VCH, Weinheim, 2008; c) K. S. Yook, J. Y. Lee, *Adv. Mater.* **2012**, *24*, 3169–3190; d) C.-F. Chang, Y.-M. Cheng, Y. Chi, Y.-C. Chiu, C.-C. Lin, G.-H. Lee, P.-T. Chou, C.-C. Chen, C.-H. Chang, C.-C. Wu, *Angew. Chem. Int. Ed.* **2008**, *47*, 4542–4545; *Angew. Chem.* **2008**, *120*, 4618–4621; e) C.-H. Yang, Y.-M. Cheng, Y. Chi, C.-J. Hsu, F.-C. Fang, K.-T. Wong, P.-T. Chou, C.-H. Chang, M.-H. Tsai, C.-C. Wu, *Angew. Chem. Int. Ed.* **2007**, *46*, 2418–2421; *Angew. Chem.* **2007**, *119*, 2470–2473; f) R. Meerheim, K. Walzer, G. He, M. Pfeiffer, K. Leo, *Proc. SPIE-Int. Soc. Opt. Eng.* **2006**, *6192*, 61920P; g) H. Xu, R. Chen, Q. Sun, W. Lai, Q. Su, W. Huang, X. Liu, *Chem. Soc. Rev.* **2014**, *43*, 3259–3302; h) C. Adachi, M. A. Baldo, M. E. Thompson, S. R. Forrest, *J. Appl. Phys.* **2001**, *90*, 5048–5051; i) X.-C. Hang, T. Fleetham, E. Turner, J. Brooks, J. Li, *Angew. Chem. Int. Ed.* **2013**, *52*, 6753–6756; *Angew. Chem.* **2013**, *125*, 6885–6888; j) T. Fleetham, G. Li, L. Wen, J. Li, *Adv. Mater.* **2014**, *26*, 7116–7121; k) P.-T. Chou, Y. Chi, *Chem. Eur. J.* **2007**, *13*, 380–395; l) J. Wang, F. Zhang, J. Zhang, W. Tang, A. Tang, H. Peng, Z. Xu, F. Teng, Y. Wang, *J. Photochem. Photobiol. C* **2013**, *17*, 69–104; m) H. Sasabe, J. Kido, *Eur. J. Org. Chem.* **2013**, 7653–7663; n) J. Chen, F. Zhao, D. Ma, *Mater. Today* **2014**, *17*, 175–183; o) P.-T. Chou, Y. Chi, M.-W. Chung, C.-C. Lin, *Coord. Chem. Rev.* **2011**, *255*, 2653–2665.

- [2] a) T. Strassner, Y. Unger, D. Meyer, O. Molt, I. Muenster, G. Wagenblast, *Inorg. Chem. Commun.* **2013**, *30*, 39–41; b) J. Li, P. I. Djurovich, B. D. Al-

leyne, M. Yousufuddin, N. N. Ho, J. C. Thomas, J. C. Peters, R. Bau, M. E. Thompson, *Inorg. Chem.* **2005**, *44*, 1713–1727; c) T. Sajoto, P. I. Djurovich, A. Tamayo, M. Yousufuddin, R. Bau, M. E. Thompson, R. J. Holmes, S. R. Forrest, *Inorg. Chem.* **2005**, *44*, 7992–8003; d) T. Sajoto, P. I. Djurovich, A. B. Tamayo, J. Oxgaard, W. A. Goddard, M. E. Thompson, *J. Am. Chem. Soc.* **2009**, *131*, 9813–9822; e) S. Lamansky, P. Djurovich, D. Murphy, F. Abdel-Razzaq, H.-E. Lee, C. Adachi, P. E. Burrows, S. R. Forrest, M. E. Thompson, *J. Am. Chem. Soc.* **2001**, *123*, 4304–4312.

- [3] M. A. Baldo, D. F. O'Brien, Y. You, A. Shoustikov, S. Sibley, M. E. Thompson, S. R. Forrest, *Nature* **1998**, *395*, 151–154.
- [4] a) A. Bossi, A. F. Rausch, M. J. Leitl, R. Czerwieniec, M. T. Whited, P. I. Djurovich, H. Yersin, M. E. Thompson, *Inorg. Chem.* **2013**, *52*, 12403–12415; b) B. Hirani, J. Li, P. I. Djurovich, M. Yousufuddin, J. Oxgaard, P. Persson, S. R. Wilson, R. Bau, W. A. Goddard, III, M. E. Thompson, *Inorg. Chem.* **2007**, *46*, 3865–3875; c) B. Ma, J. Li, P. I. Djurovich, M. Yousufuddin, R. Bau, M. E. Thompson, *J. Am. Chem. Soc.* **2005**, *127*, 28–29; d) J. Brooks, Y. Babayan, S. Lamansky, P. I. Djurovich, I. Tsypa, R. Bau, M. E. Thompson, *Inorg. Chem.* **2002**, *41*, 3055–3066; e) D. N. Kozhevnikov, V. N. Kozhevnikov, M. M. Ustinova, A. Santoro, D. W. Bruce, B. Koenig, R. Czerwieniec, T. Fischer, M. Zabel, H. Yersin, *Inorg. Chem.* **2009**, *48*, 4179–4189.
- [5] a) J. A. G. Williams, A. Beeby, E. S. Davies, J. A. Weinstein, C. Wilson, *Inorg. Chem.* **2003**, *42*, 8609–8611; b) A. F. Rausch, L. Murphy, J. A. G. Williams, H. Yersin, *Inorg. Chem.* **2012**, *51*, 312–319; c) E. Rossi, L. Murphy, P. L. Brothwood, A. Colombo, C. Dragonetti, D. Roberto, R. Ugo, M. Cocchi, J. A. G. Williams, *J. Mater. Chem.* **2011**, *21*, 15501–15510; d) E. Rossi, A. Colombo, C. Dragonetti, D. Roberto, R. Ugo, A. Valore, L. Falcioia, P. Brulatti, M. Cocchi, J. A. G. Williams, *J. Mater. Chem.* **2012**, *22*, 10650–10655.
- [6] a) M. Egen, K. Kahle, M. Bold, T. Gessner, C. Lennartz, S. Nord, H.-W. Schmidt, M. Thelakkat, M. Baete, C. Neuber, W. Kowalsky, C. Schildknecht, H.-H. Johannes, WO 2006056418A2, **2006**; b) X. Zhang, A. M. Wright, N. J. DeYonker, T. K. Hollis, N. I. Hammer, C. E. Webster, E. J. Valente, *Organometallics* **2012**, *31*, 1664–1672; c) R. Visbal, M. C. Gimeno, *Chem. Soc. Rev.* **2014**, *43*, 3551–3574.
- [7] a) Z. M. Hudson, C. Sun, M. G. Helander, Y.-L. Chang, Z.-H. Lu, S. Wang, *J. Am. Chem. Soc.* **2012**, *134*, 13930–13933; b) A. Tronnier, S. Metz, G. Wagenblast, I. Muenster, T. Strassner, *Dalton Trans.* **2014**, *43*, 3297–3305; c) A. Tronnier, N. Nischan, S. Metz, G. Wagenblast, I. Muenster, T. Strassner, *Eur. J. Inorg. Chem.* **2014**, *256*–264; d) A. Tronnier, A. Poethig, E. Herdtweck, T. Strassner, *Organometallics* **2014**, *33*, 898–908; e) A. Tronnier, A. Poethig, S. Metz, G. Wagenblast, I. Muenster, T. Strassner, *Inorg. Chem.* **2014**, *53*, 6346–6356; f) A. Tronnier, A. Risler, N. Langer, G. Wagenblast, I. Muenster, T. Strassner, *Organometallics* **2012**, *31*, 7447–7452; g) A. Tronnier, T. Strassner, *Dalton Trans.* **2013**, *42*, 9847–9851.
- [8] a) A. Tronnier, N. Nischan, T. Strassner, *J. Organomet. Chem.* **2013**, *730*, 37–43; b) A. Tronnier, D. Schleicher, T. Strassner, *J. Organomet. Chem.* **2015**, *775*, 155–163; c) M. Tenne, S. Metz, I. Muenster, G. Wagenblast, T. Strassner, *Organometallics* **2013**, *32*, 6257–6264.
- [9] Y. Unger, D. Meyer, O. Molt, C. Schildknecht, I. Muenster, G. Wagenblast, T. Strassner, *Angew. Chem. Int. Ed.* **2010**, *49*, 10214–10216; *Angew. Chem.* **2010**, *122*, 10412–10414.
- [10] T. Shigehiro, S. Yagi, T. Maeda, H. Nakazumi, H. Fujiwara, Y. Sakurai, *J. Phys. Chem. C* **2013**, *117*, 532–542.
- [11] M. Tenne, Y. Unger, T. Strassner, *Acta Crystallogr. Sect. C* **2012**, *68*, m203–m205.

Received: May 28, 2015

Published online on July 27, 2015